

1 **Title: BOLD cerebrovascular reactivity MRI to identify tissue reperfusion failure after**
2 **EVT in patients with LVO acute stroke**

3 **Authors:** Jacopo Bellomo, MD^{1,2}; Martina Sebök, MD PhD^{1,2}; Vittorio Stumpo, MD^{1,2};
4 Christiaan HB van Niftrik, MD PhD^{1,2}; Darja Meisterhans, BMed^{1,2}; Marco Piccirelli, PhD^{2,3};
5 Lars Michels, PhD^{2,3}; Beno Reolon, BMed^{2,3}; Tilman Schubert, MD^{2,3}; Zsolt Kulcsar, MD^{2,3};
6 Andreas R Luft, MD^{2,4,5}; Susanne Wegener, MD^{2,4}; Luca Regli, MD^{1,2}; Jorn Fierstra, MD
7 PhD^{1,2}

8 **Affiliations:**

9 ¹Department of Neurosurgery, University Hospital Zurich, Zurich, Switzerland

10 ²Clinical Neuroscience Center, University of Zurich and Swiss Federal Institute of
11 Technology Zurich, Zurich, Switzerland

12 ³Department of Neuroradiology, University Hospital Zurich, Zurich, Switzerland

13 ⁴Department of Neurology, University Hospital Zurich, Zurich, Switzerland

14 ⁵cereneo Center for Neurology and Rehabilitation, Vitznau, Switzerland

15

16 **Corresponding author: Jacopo Bellomo**

17 Department of Neurosurgery

18 University Hospital Zurich, Zurich, Switzerland

19 Frauenklinikstrasse 10, CH-8091 Zurich

20 Email: jacopo.bellomo@usz.ch

21 **Authorship contributions:**

22 Data collection and curation: J.B., M.S., V.S., CHB.V., D.M.

23 Analysis of the data and preparing the manuscript draft: J.B., J.F.

24 Revising the manuscript: all authors

25 Supervising the study: J.F., S.W., A.L.

26 All authors approved the final manuscript version.

27

28 **Total word count of the manuscript: 5272 words**

29

30

31

32

33

34

35 **ABSTRACT**

36 **Background and purpose:** In acute ischemic stroke due to large-vessel occlusion (LVO), the
37 clinical outcome after endovascular thrombectomy (EVT) is influenced by the extent of
38 autoregulatory hemodynamic impairment and collateral recruitment, which can be derived
39 from blood oxygenation-level dependent cerebrovascular reactivity (BOLD-CVR). BOLD-
40 CVR imaging identifies brain areas influenced by hemodynamic steal. We sought to
41 investigate the presence of steal phenomenon and its relationship to DWI lesions and clinical
42 deficit in the acute phase of ischemic stroke following successful vessel recanalization.

43 **Methods:** From the prospective longitudinal IMPreST (Interplay of Microcirculation and
44 Plasticity after ischemic Stroke) cohort study, patients with acute ischemic unilateral LVO
45 stroke of the anterior circulation with successful endovascular thrombectomy (EVT; mTICI
46 scale $\geq 2b$) and subsequent BOLD-CVR examination were included for this analysis. We
47 analyzed the spatial correlation between brain areas exhibiting BOLD-CVR associated steal
48 phenomenon and DWI infarct lesion as well as the relationship between steal phenomenon
49 and NIHSS score at hospital discharge.

50 **Results:** Included patients (n=21) exhibited steal phenomenon to different extents, whereas
51 there was only a partial spatial overlap with the DWI lesion (median 18.51%; IQR, 8.44-
52 59.09). The volume of steal phenomenon outside the DWI lesion showed a positive
53 correlation with overall DWI lesion volume and was a significant predictor for the NIHSS
54 score at hospital discharge.

55 **Conclusions:** Patients with acute ischemic unilateral LVO stroke exhibited hemodynamic
56 steal identified by BOLD-CVR after successful EVT. Steal volume was associated with DWI
57 infarct lesion size and with poor clinical outcome at hospital discharge. BOLD-CVR may
58 further aid in better understanding persisting hemodynamic impairment following reperfusion
59 therapy.

60 **Keywords:** ischemic stroke; large-vessel occlusion; cerebrovascular reactivity; steal
61 phenomenon; BOLD-CVR; DWI; endovascular thrombectomy; reperfusion failure.

62 **Abbreviations:** LVO = large-vessel occlusion; BOLD = blood oxygen-level dependent; MRI
63 = magnetic resonance imaging; CVR = cerebrovascular reactivity; DWI = diffusion-weighted
64 imaging; EVT = endovascular thrombectomy; NIHSS = National Institutes of Health Stroke
65 Scale; mTICI = modified Thrombolysis In Cerebral Infarction; IMPreST = Interplay of
66 Microcirculation and Plasticity after ischemic Stroke; SD = standard deviation; SE = standard
67 error.

68

69

70

71

72

73

74

75

76

77

78

79

80

81

82

83

84

85

86

87

88

89 INTRODUCTION

90 Acute ischemic large-vessel occlusion (LVO) stroke is characterized by proximal occlusion of
91 a large cerebral vessel (e.g., internal carotid artery or middle cerebral artery) and has a
92 profound hemodynamic impact on distal brain tissue, i.e., hypoperfusion and tissue ischemia.¹
93 Hypoperfusion and consecutive tissue damage is a dynamic process in the acute ischemic
94 phase which is influenced by collateral recruitment and autoregulation.¹⁻⁴ Timely restoration
95 of cerebral blood flow by endovascular thrombectomy (EVT) is the most effective maneuver
96 for salvaging ischemic brain tissue that is not already irreversibly lost.⁵⁻⁸ However, in some
97 cases no improvement or even worsening of clinical status despite successful vessel
98 recanalization can be observed. It is hypothesized that the mechanisms underlying this
99 reperfusion failure are attributable to remaining macro- and/or microvascular dysfunction and
100 subsequent persisting hemodynamic impairment within the ischemic territory.⁹⁻¹¹

101 In recent years, several neuroimaging techniques have been employed investigating
102 microvasculature and hemodynamic tissue responses following acute ischemia and
103 subsequent endovascular revascularization to predict tissue fate.^{10,12,13} Hyper- and
104 hypoperfusion tissue status observed with perfusion-weighted magnetic resonance imaging
105 (MRI) have been both associated with poor clinical outcome. For instance, hypoperfusion
106 despite successful EVT is thought to result from insufficient capillary reflow induced by
107 different mechanisms (e.g. microvascular occlusion with microclots or neutrophils)¹³⁻¹⁶.
108 Hyperperfusion, most likely, comes from persisting altered cerebrovascular
109 autoregulation^{13,17}. A better characterization of hemodynamic tissue state in these patients
110 would help to further understand the mechanisms underlying reperfusion failure.

111 Blood oxygenation-level dependent cerebrovascular reactivity (BOLD-CVR) may be suited as
112 an emerging, clinically applicable, hemodynamic imaging technique capable to evaluate
113 vessel reactivity and remaining vasodilatory reserve as the result of flow redistribution under

114 a controlled hypercapnic challenge.¹⁸⁻²⁰ Of particular interest are brain areas exhibiting
115 BOLD-CVR associated steal phenomenon in the post-reperfusion period, indicating persisting
116 severely impaired cerebrovascular autoregulatory loss and insufficient collateral
117 compensatory activation.^{21,22} Recently, we have enabled a clinical infrastructure for advanced
118 MRI investigations in patients presenting with acute ischemic unilateral LVO stroke after
119 reperfusion therapy (IMPreST prospective cohort study, <https://www.stroke.uzh.ch/en.html>).

120 We therefore studied the presence of BOLD-CVR identified steal, i.e., a paradoxical BOLD
121 signal drop during hypercapnia¹⁹, and its association with diffusion-weighted imaging (DWI)
122 lesions, as well as clinical outcome after acute ischemic unilateral LVO stroke following
123 successful endovascular thrombectomy.

124 **MATERIALS AND METHODS**

125 Study population

126 From the prospective IMPreST (Interplay of Microcirculation and Plasticity after ischemic
127 Stroke) longitudinal observational cohort study, we selected all patients with acute ischemic
128 unilateral LVO stroke of the anterior circulation that were successfully treated with EVT
129 (modified Thrombolysis In Cerebral Infarction - mTICI - scale ≥ 2 ²³) and received BOLD-
130 CVR examination. The IMPreST study is a prospective study designed to explore the
131 correlation between different imaging modalities for microcirculation and its association with
132 clinical outcome in patients with acute ischemic unilateral LVO stroke. Inclusion criteria
133 were: (1) ≤ 72 hours first-ever clinical ischemic stroke at hospital admission; (2) occlusion of
134 M1/M2-segment of the middle cerebral artery, and/or intracranial internal carotid artery, and
135 perfusion deficits with cortical involvement; (3) 18 years or above; (4) living independent
136 before stroke (modified Ranking Scale - mRS - ≤ 3 ²⁴); (5) written informed consent of the
137 patient or when the patient is not able to participate in the consenting procedure, the written
138 authorization of an independent doctor who is not involved in the research project to

139 safeguard the interests of the patients (in that case, post-hoc written informed consent of the
140 patient or next of kin had to be obtained). Exclusion criteria were: (1) major cardiac,
141 psychiatric and/or neurological diseases; (2) early seizures; (3) known or suspected non-
142 compliance, drug and/or alcohol abuse; (4) contra-indications for MRI; (5) documented
143 evidence that the patient does not want to participate in any scientific study. Included patients
144 received standard multimodality MRI at predefined time points (i.e., ≤ 72 hours, at day 7 ± 3 ,
145 at day 90 ± 14) from stroke symptom onset. The exact scanning protocol can be reviewed in
146 the **Supplementary material** section. For this work, we considered only BOLD-CVR and
147 DWI data acquired during the first examination session (i.e., ≤ 72 hours from stroke symptom
148 onset).

149 Ethics

150 The research ethic committee of the Canton Zurich, Switzerland (Kantonale Ethikkommission
151 Zürich; KEK-ZH-NR. 2019-00750) approved the IMPreST prospective observational cohort
152 study. Written informed consent was obtained from each participant before inclusion. The
153 study was conducted in accordance with the ethical standards as laid down in the 1964
154 Declaration of Helsinki and its later amendments.

155 Image acquisition protocol

156 The imaging study was performed at 3-Tesla Skyra MRI scanner (Siemens Healthineers,
157 Forchheim, Germany) with a 32-channel head matrix coil after the patients have been enrolled
158 in the study. The imaging protocol included diffusion-weighted imaging (DWI) [2D EPI
159 sequence, repetition and echo time (TR/TE) = 2500/75 ms, flip angle = 90° , slice thickness
160 (ST) = 5 mm, b -values = B0 and B1000 s/mm²], BOLD imaging [2D EPI sequence, TR/TE =
161 2000/30 ms, flip angle = 85° , bandwidth 2368 Hz/Px, and field of view (FOV) 192x192
162 mm²], 3D T1-MPRAGE imaging [TR/TE = 2200/5.14 ms, flip angle 8° , ST 1 mm, FOV
163 230x230 mm²]. During the BOLD MRI sequence, a standardized carbon dioxide (CO₂)

164 stimulus was applied using the RespirAct™ (Thornhill Research Institute, Toronto, Canada),
165 that allows for precise CO₂ end-tidal pressure (P_{et}CO₂) targeting while maintaining normal
166 levels of O₂ (iso-oxia).²⁵ Our standardized CO₂ protocol consisted of an initial 100 s at the
167 patient-specific resting P_{et}CO₂, after which P_{et}CO₂ was increased of 10 mmHg for 80 s, and a
168 return to resting P_{et}CO₂ for 120 s; P_{et}O₂ was maintained at the patient-specific resting value
169 for the entire duration of the examination.

170 As specified above, BOLD-CVR imaging and DWI data were collected in a single
171 examination session within 72 hours from stroke symptom onset. The quality of the single
172 BOLD-CVR imaging data was evaluated considering head motion artifacts and the
173 consistency of the CO₂ stimulus. Specifically, examination were discarded from our analysis
174 if the mean frame-wise displacement between adjacent acquisition volumes was > 2 mm²⁶ or
175 if the CO₂ step change was < 6 mmHg.

176 Image processing

177 Morphological and functional images were first processed singularly to calculate parameter
178 maps. BOLD-CVR maps were obtained according to the previously described Zurich analysis
179 pipeline²⁷ using MATLAB2019 (The MathWorks, Inc., Natick, United States) and SPM12
180 (Wellcome Trust Centre for Neuroimaging, Institute of Neurology, University College
181 London). BOLD-CVR was calculated voxel-per-voxel as percentage of BOLD signal change
182 divided by the absolute change in P_{et}CO₂ (% ΔBOLD/mmHg). Apparent diffusion coefficient
183 (ADC) maps were automatically calculated from DWI data. All the resulting maps were then
184 co-registered to the individual anatomical T1 space (intra-individual co-registration) using
185 SPM12. Lastly, we extrapolated quantitative values from the co-registered parameter maps for
186 different region of interests (ROIs) - i.e., whole brain (WB), grey matter (GM) and white
187 matter (WM), ipsilateral and contralateral hemisphere, and major vascular territories (anterior
188 cerebral artery, ACA; middle cerebral artery, MCA; posterior cerebral artery, PCA). ROIs of

189 the vascular territories were provided by the recently published atlases by Liu et al.²⁸ To
190 better investigate brain areas under steal, we selected for each patient the relevant voxels
191 showing negative response in the BOLD-CVR map. First, we considered all voxels with $< 0\%$
192 BOLD signal change/mmHg CO₂. Then, using our healthy atlas as reference, a Z-score map²⁹
193 of the BOLD-CVR map was generated and the voxels with Z-score < 2 were excluded. In this
194 way, only those negative voxels that differed significantly from the healthy cohort were
195 considered (**Supplementary Figure 1**). Additionally, for each patient the deep learning-based
196 algorithm by Liu et al. was used to automatically segment stroke lesion from DWI data (DWI
197 infarct stroke lesion).³⁰

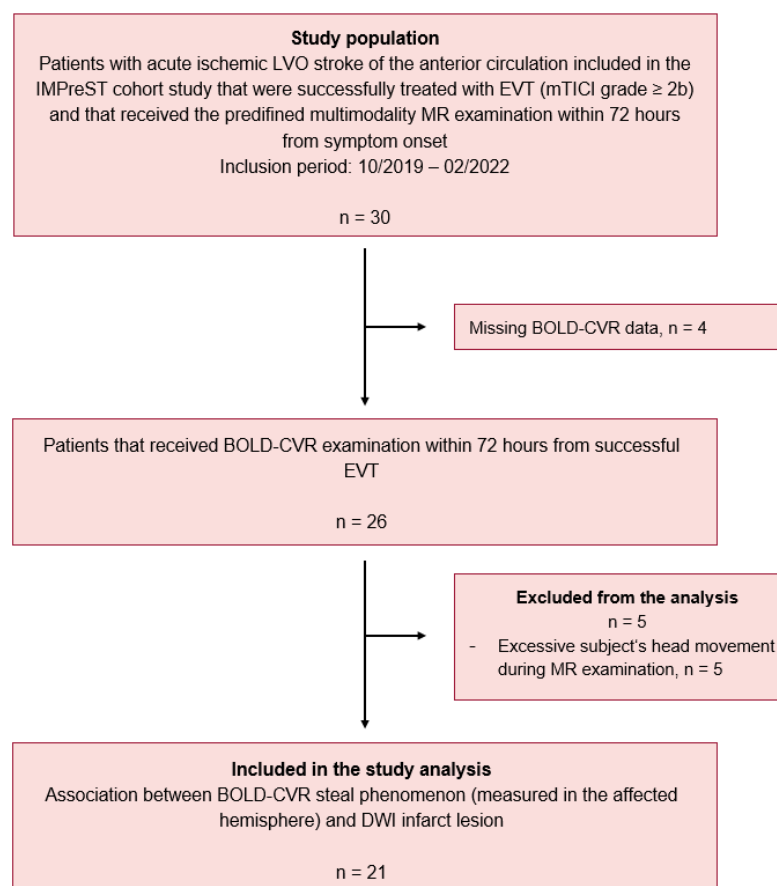
198 Statistical analysis

199 The statistical analysis of this study was carried out with the statistical program *R studio*
200 (Posit Software, PBC formerly R Studio, version 02.07.2022). First, we described for each
201 patient the mean BOLD-CVR values as well as the volumetric distribution of BOLD-CVR
202 associated steal phenomenon in the different vascular territories and within the DWI infarct
203 stroke lesion. Secondly, we looked at the spatial correlation between BOLD-CVR associated
204 steal phenomenon and DWI infarct lesion by calculating the percentage of tissue exhibiting
205 steal phenomenon that was also included in the infarct lesion. We defined therefore DWI-
206 positive steal phenomenon-positive respectively DWI-negative steal phenomenon-positive
207 brain tissue areas, and we performed a Spearman's correlation analysis to study the partial
208 correlation between DWI-negative steal phenomenon-positive brain tissue and DWI infarct
209 lesion with symptom-to-MR time (in hour, defined as time between stroke symptom onset and
210 baseline MR study session), age and pre-thrombectomy NIHSS values as confounding
211 variables (covariates). Lastly, we modeled a multivariable linear regression model to study the
212 effect of the presence of DWI-negative steal-positive brain tissue on NIHSS values at

213 discharge with DWI lesion volumes, pre-thrombectomy NIHSS values, and age as
214 confounding variables (covariates).

215 RESULTS

216 Between October 2019 and February 2022, twenty-six patients with acute ischemic unilateral
217 LVO stroke consecutively included in the IMPreST prospective study received BOLD-CVR
218 examination within 72 hours from stroke symptom onset. Of these, 5 patients were excluded
219 due to excessive head movement during MR examination. Twenty-one patients were included
220 in analysis (**Figure 1**) and their baseline characteristics can be reviewed in **Table 1**.



221

222

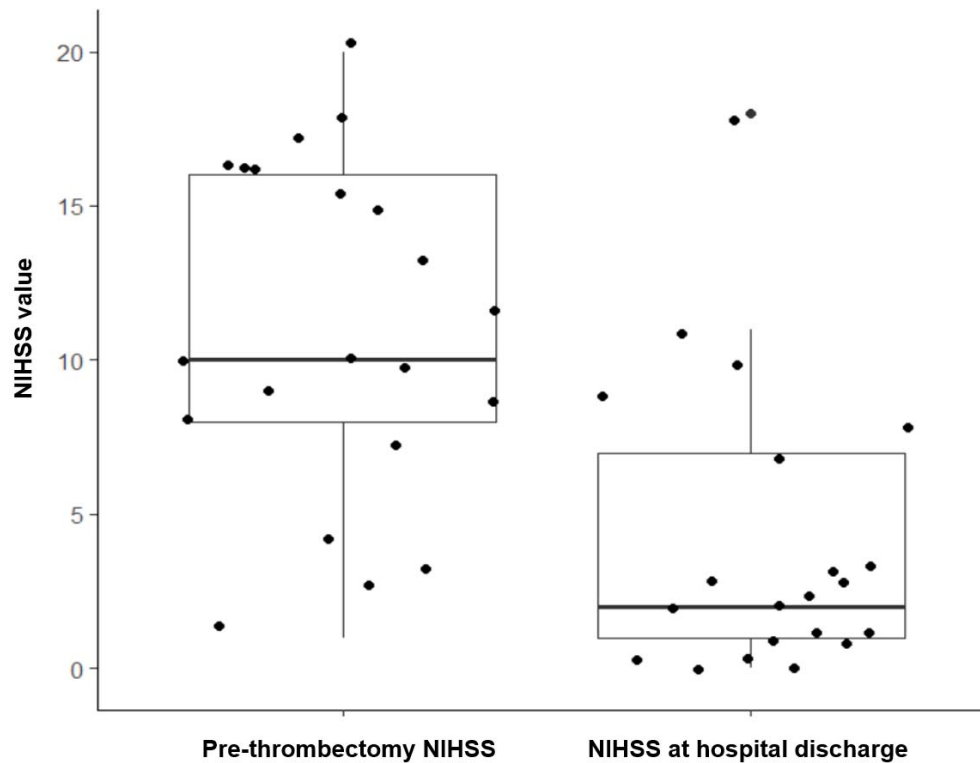
Figure 1. Study flow chart.

223 LVO indicates large-vessel occlusion stroke; IMPreST, Interplay of Microcirculation and
224 Plasticity after ischemic Stroke; EVT, endovascular thrombectomy; mTICI, modified
225 Thrombolysis in Cerebral Infarction; MR, magnetic resonance; BOLD-CVR, blood oxygen
226 level dependent cerebrovascular reactivity; DWI, diffusion-weighted imaging.

227

228 In the MR examination session after successful reperfusion therapy, we found high variability
229 of the presence of steal phenomenon in the affected MCA and ACA territory of the included
230 patients, with a median volume of 21.58 mL (IQR, 7.68-64.11). **Table 2** summarizes the
231 volumetric distribution of BOLD-CVR steal for all the included patients. Interestingly, steal-
232 affected regions were heterogeneously distributed both within and outside the DWI lesion. On
233 average, only 18.51% (INR, 8.44-59.09) of DWI lesion overlapped the steal area; respectively
234 only 26.31% (IQR, 13.84-39.47) of steal volume was part of the DWI lesion (**Supplementary**
235 **Figure 2**). Within the DWI lesion, on average, severely impaired BOLD-CVR values were
236 observed (mean \pm SD; $0.042 \pm 0.058 \Delta\text{BOLD\%/mmHg}$). A Spearman's correlation analysis
237 showed a positive partial correlation (correlation coefficient 0.64; SE 0.20; *P* value 0.004)
238 between DWI lesion volume and BOLD-CVR steal volume found outside the stroke lesion
239 after correcting for possible confounding variables (age, symptom-to-MR time, and NIHSS
240 baseline values).

241 At hospital discharge the median NIHSS score value was 2.00 (IQR, 1.00-7.25). Five-teen
242 patients had a NIHSS score equal or less than 3 (median, min-max; 1, 0-3), the remaining six
243 patients more than 3 (median, min-max; 9.50, 7.00-18.00). A comparison of NIHSS values at
244 hospital admission (pre-thrombectomy) and at hospital discharge are presented in **Figure 2**.



245

246

Figure 2. Boxplot of NIHSS score measurements over time.

247

NIHSS indicates National Institutes of Health Stroke Scale.

248

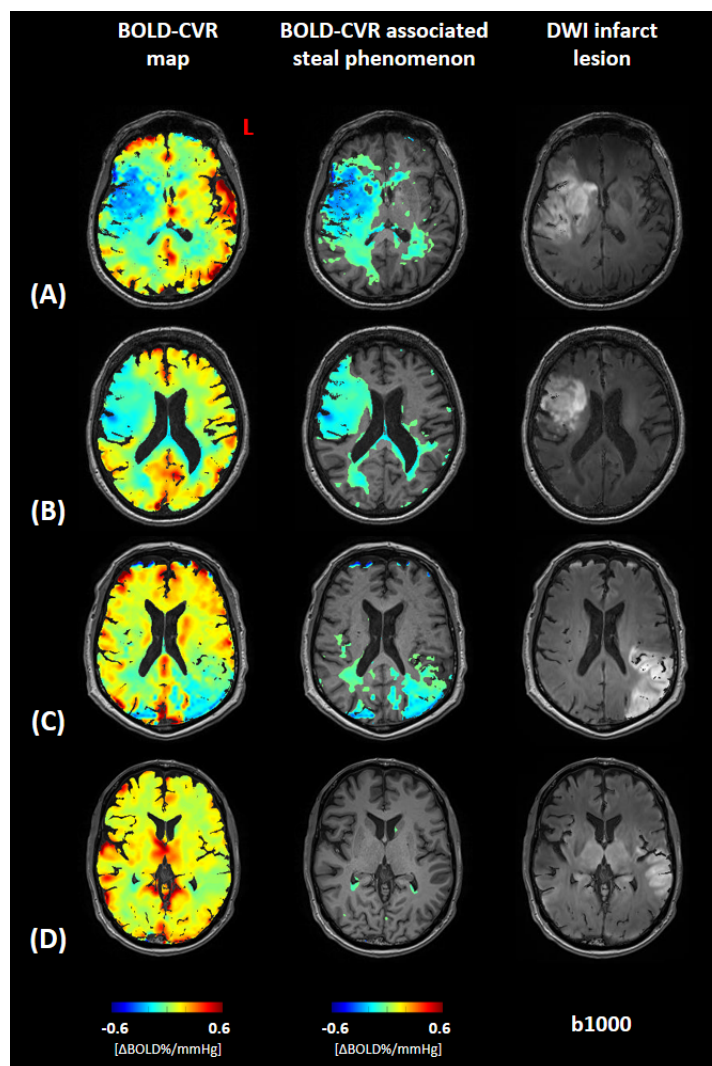
249 A multivariable linear regression model (**Table 3**) showed that the volume of BOLD-CVR

250 defined steal found outside the DWI lesion was a significant predictor for the NIHSS score at

251 discharge (regression coefficient β 0.07, SE 0.03, *P* value 0.034) after correcting for DWI

252 lesion size, pre-thrombectomy NIHSS values, and age (adjusted R^2 0.64, *P* value <0.001). In

253 **Figure 3**, BOLD-CVR and DWI findings of four example patients are presented.



254

255 **Figure 3. Association between BOLD-CVR associated steal phenomenon and DWI**
256 **infarct lesion.**

257 Blood oxygen level dependent cerebrovascular reactivity (BOLD-CVR) and trace DWI
258 (diffusion-weighted imaging) map of four illustrative examples are presented. For each
259 patient a whole-brain BOLD-CVR map, a BOLD-CVR showing only steal phenomenon
260 tissue areas, and trace DWI map are depicted. **A**, male subject (age range: 66-70 years)
261 showing 97.12 mL infarct lesion in the middle cerebral artery (MCA) territory right, showing
262 a total of 189.76 mL steal phenomenon, 73.84 mL within and 115.52 mL outside the infarct
263 lesion. NIHSS 16 at hospital admission, NIHSS 9 at hospital discharge. **B**, female subject (age
264 range: 66-70 years) showing 52.84 mL infarct lesion in the MCA territory right, showing a
265 total of 113.19 mL steal phenomenon, 46.55 mL within and 66.64 mL outside the infarct
266 lesion. NIHSS 12 at hospital admission, NIHSS 10 at hospital discharge. **C**, male subject (age
267 range: 71-75 years) showing 89.57 mL infarct lesion in the MCA territory left, showing a total
268 of 83.99 mL steal phenomenon, 51.79 mL within and 32.20 mL outside the infarct lesion.
269 NIHSS 10 at hospital admission, NIHSS 1 at hospital discharge. **D**, male subject (age range:
270 66-70 years) showing 47.15 mL infarct lesion in the MCA territory left, showing a total of
271 4.40 mL steal phenomenon, 0.70 mL within and 3.70 mL outside the infarct lesion. NIHSS 3
272 at hospital admission, NIHSS 1 at hospital discharge.

273

274 **DISCUSSION**

275 Our study shows that BOLD-CVR associated steal phenomenon can be detected in the
276 affected hemisphere of patients with acute ischemic unilateral LVO stroke despite successful
277 EVT, which may indicate reperfusion failure. Brain areas with steal phenomenon only
278 showed a partial spatial agreement with DWI infarct lesions, whereas steal phenomenon was
279 also observed in brain tissue outside the DWI lesion. The brain tissue volume exhibiting steal
280 phenomenon outside the infarct – DWI – lesion correlated strongly with the volume of DWI
281 derived infarct lesion and was a significant predictor for a poorer clinical status at hospital
282 discharge.

283 To the best of our knowledge, we could not identify similar studies measuring CVR after
284 acute reperfusion therapy in a similar cohort of patients, and therefore a direct comparison of
285 our results with already existing findings is not possible to date. However, some clinical
286 studies reported the findings observed with other imaging techniques.^{31–35} A dynamic growth
287 of DWI lesion after revascularization procedures has been observed reflecting reperfusion
288 failure.^{31,35} Infarct growth contributes to the final infarct volume, correlates with clinical
289 outcome and has been associated with DWI lesion size pre-EVT as well as mTICI grade < 2b
290 and hypoperfusion post-EVT.³¹ These findings enhance the importance of identifying
291 prognostic factors that are associated with reperfusion failure and can therefore predict infarct
292 lesion evolution after EVT. A recent work of Potreck et al.³³ studied tissue response after
293 successful EVT with combined perfusion and permeability MR imaging and showed distinct
294 post-reperfusion pathophysiological tissue responses that were associated with different
295 clinical courses. In general, hypoperfusion occurred more often in patients with unfavourable
296 clinical outcome compared to hyperperfusion or unchanged perfusion. BOLD-CVR imaging,
297 thanks to its capability to study vessel reactivity, offers the potential to provide additional
298 information about microvascular functionality. We focused our analysis on brain regions

299 exhibiting BOLD-CVR identified steal because we thought this could represent irreversible
300 tissue damage and/or brain areas subjected to reperfusion failure. Based on the current
301 knowledge on the pathophysiological mechanisms of reperfusion failure^{9,14,16}, we
302 hypothesized that steal phenomenon could reflect on of the following: (1) exhausted regional
303 vasodilatory reserve induced by microvascular occlusion with microclots, microvascular
304 occlusion with recruited neutrophils, and/or vessel constriction; (2) loss of cerebrovascular
305 autoregulation. Most of the knowledge about reperfusion failure mechanisms came from pre-
306 clinical studies. Recently, Binder et al.³⁶ investigated the role of leptomeningeal collaterals in
307 reperfusion failure in a rodent stroke model and reported a loss of vascular tone (i.e., loss of
308 autoregulation) in the distal MCA branch segments after reperfusion which was associated
309 with a worse clinical outcome.

310 In our study, we observed a partial spatial agreement between DWI infarct lesion and BOLD-
311 CVR identified steal. We can distinguish three different tissue areas: DWI-positive steal-
312 negative brain tissue, DWI-positive steal-positive brain tissue, and DWI-negative steal-
313 positive brain tissue. In the DWI infarct lesion (“DWI-positive”), both steal phenomenon and
314 impaired, but maintained BOLD-CVR values were observed. Two possible explanations to
315 this finding seem plausible: (1) infarcted necrotic tissue included in the DWI lesion represents
316 tissue with disrupted vessels (i.e., no cerebrovascular reactivity) and therefore shows BOLD-
317 CVR around zero with either slightly positive or slightly negative values³⁷; (2) a part of the
318 DWI lesion represents cerebral tissue not yet irreversible damaged that shows maintained
319 cerebrovascular reactivity after successful reperfusion^{35,38}. Of major clinical relevance we
320 observed tissue exhibiting a steal phenomenon that was not included in the DWI lesion
321 (“DWI-negative”), which could indicate tissue not irreversibly damaged but with severely
322 impaired hemodynamic characteristics. We found a positive correlation of this DWI-negative
323 steal-positive brain tissue with DWI infarct lesion size and a significant association with
324 higher NIHSS clinical score at hospital discharge. These findings indirectly support what we

325 assumed in the beginning, namely, that the steal phenomenon does not reflect just infarcted
326 tissue and that the identified DWI-negative steal-positive region could depict brain tissue with
327 microvascular dysfunction (i.e., reperfusion failure) that could evolve to an irreversibly
328 infarcted area.

329 Future directions

330 Our preliminary findings highlight the potential of BOLD-CVR imaging as a novel technique
331 to characterize brain tissue hemodynamic responses after EVT. Future research, however, is
332 needed to further understand the link between the observed BOLD-CVR steal phenomenon
333 and reperfusion failure and its association with clinical outcome. A correlation analysis
334 between BOLD-CVR findings and MR perfusion parameters (i.e., cerebral blood flow, CBF,
335 cerebral blood volume, CBV, mean transit time, MTT, time-to-maximum, T_{max}) could be
336 performed to confirm our hypothesis of the mechanisms behind steal phenomenon observed
337 in reperfused tissue (i.e., both loss of autoregulation with associated hyperperfusion and
338 microvascular occlusion/constriction with associated hypoperfusion). In addition, a
339 retrospective analysis to identify which pre-thrombectomy clinical/imaging factors are
340 associated with the occurrence of steal phenomenon could be considered.

341 Strength and limitations

342 This work represents a preliminary analysis of BOLD-CVR findings in a well-defined cohort
343 of patients with acute ischemic unilateral LVO stroke. The investigated imaging modalities
344 (BOLD-CVR and DWI) were acquired within the same examination session and therefore
345 high intra-subject comparability between imaging data can be assumed. However, this study
346 has some limitations. First, the small sample size of the studied cohort limited the
347 generalizability of our analysis and therefore further studies including more patients are
348 necessary to confirm our observations. Second, to avoid unethical diagnostic delay, our study
349 did not provide imaging data about tissue state before reperfusion therapy. Therefore, the

350 clinical meaning of BOLD-CVR identified steal before EVT is unknown. Third, we created a
351 steal phenomenon mask from the BOLD-CVR magnitude maps selecting all the voxel
352 exhibiting a negative response to the hypercapnic stimulus. However, the clinical relevance of
353 this steal phenomenon mask has not yet been investigated and other definitions based on
354 different thresholds respectively considering also more technical imaging aspects (e.g.,
355 contrast-to-noise ratio) should be also evaluated in the future.

356 **CONCLUSIONS**

357 Patients with unilateral acute ischemic large-vessel occlusion stroke exhibit BOLD-CVR
358 associated steal in the early phase despite successful EVT. Steal volume was associated with
359 DWI lesion size, and with poor clinical outcome at hospital discharge. The BOLD-CVR
360 identified steal phenomenon may provide a better understanding of persisting hemodynamic
361 impairment following reperfusion therapy.

362

363

364

365

366

367

368

369

370

371

372

373

374 **ACKNOWLEDGMENTS, SOURCES OF FUNDING, DISCLOSURES**

375 **Sources of Funding:** This project was funded by the Clinical Research Priority Program of
376 the University of Zurich (UZH CRPP Stroke), the Swiss National Science Foundation
377 (PP00P3_170683), the Swiss Cancer Research Foundation (KFS-3975-082016-R), and the
378 Theodor und Ida Herzog-Egli-Stiftung.

379 **Disclosures:** none.

380

381

382

383

384

385

386

387

388

389

390

391

392

393

394

395

396

397

398

399

400 **Supplemental Material**

401 Figures S1-S2

402 Supplemental methods

403

404 REFERENCES

- 405 1. Muir KW, Buchan A, von Kummer R, Rother J, Baron JC. Imaging of acute stroke.
406 *Lancet Neurol.* 2006;5(9):755-768. doi:10.1016/S1474-4422(06)70545-2
- 407 2. Seifert K, Heit JJ. Collateral Blood Flow and Ischemic Core Growth. *Transl Stroke Res.*
408 2023;14(1):13-21. doi:10.1007/s12975-022-01051-2
- 409 3. Seners P, Yuen N, Mlynash M, et al. Quantification of Penumbra Volume in
410 Association With Time From Stroke Onset in Acute Ischemic Stroke With Large Vessel
411 Occlusion. *JAMA Neurol.* Published online March 20, 2023:e230265.
412 doi:10.1001/jamaneurol.2023.0265
- 413 4. Sebök M, Esposito G, Niftrik CHB van, et al. Flow augmentation STA-MCA bypass
414 evaluation for patients with acute stroke and unilateral large vessel occlusion: a proposal
415 for an urgent bypass flowchart. *J Neurosurg.* Published online January 7, 2022:1-9.
416 doi:10.3171/2021.10.JNS21986
- 417 5. Powers WJ, Rabinstein AA, Ackerson T, et al. Guidelines for the Early Management of
418 Patients With Acute Ischemic Stroke: 2019 Update to the 2018 Guidelines for the Early
419 Management of Acute Ischemic Stroke: A Guideline for Healthcare Professionals From
420 the American Heart Association/American Stroke Association. *Stroke.*
421 2019;50(12):e344-e418. doi:10.1161/STR.0000000000000211
- 422 6. Hankey GJ. Stroke. *Lancet Lond Engl.* 2017;389(10069):641-654. doi:10.1016/S0140-
423 6736(16)30962-X
- 424 7. Malik P, Anwar A, Patel R, Patel U. Expansion of the dimensions in the current
425 management of acute ischemic stroke. *J Neurol.* 2021;268(9):3185-3202.
426 doi:10.1007/s00415-020-09873-6
- 427 8. Olthuis SGH, Pirson FAV, Pinckaers FME, et al. Endovascular treatment versus no
428 endovascular treatment after 6-24 h in patients with ischaemic stroke and collateral flow
429 on CT angiography (MR CLEAN-LATE) in the Netherlands: a multicentre, open-label,
430 blinded-endpoint, randomised, controlled, phase 3 trial. *Lancet Lond Engl.* Published
431 online March 29, 2023:S0140-6736(23)00575-5. doi:10.1016/S0140-6736(23)00575-5
- 432 9. El Amki M, Wegener S. Improving Cerebral Blood Flow after Arterial Recanalization:
433 A Novel Therapeutic Strategy in Stroke. *Int J Mol Sci.* 2017;18(12):2669.
434 doi:10.3390/ijms18122669
- 435 10. Nie X, Leng X, Miao Z, Fisher M, Liu L. Clinically Ineffective Reperfusion After
436 Endovascular Therapy in Acute Ischemic Stroke. *Stroke.* 2023;54(3):873-881.
437 doi:10.1161/STROKEAHA.122.038466
- 438 11. Lee JS, Bang OY. Collateral Status and Outcomes after Thrombectomy. *Transl Stroke*
439 *Res.* 2023;14(1):22-37. doi:10.1007/s12975-022-01046-z

- 440 12. Zhang Z, Pu Y, Mi D, Liu L. Cerebral Hemodynamic Evaluation After Cerebral
441 Recanalization Therapy for Acute Ischemic Stroke. *Front Neurol.* 2019;10:719.
442 doi:10.3389/fneur.2019.00719
- 443 13. N van der K, Baa F, Cblm M, A van der L, Rm D. Implications of Post-recanalization
444 Perfusion Deficit After Acute Ischemic Stroke: a Scoping Review of Clinical and
445 Preclinical Imaging Studies. *Transl Stroke Res.* Published online January 19, 2023.
446 doi:10.1007/s12975-022-01120-6
- 447 14. Okada Y, Copeland BR, Fitridge R, Koziol JA, del Zoppo GJ. Fibrin contributes to
448 microvascular obstructions and parenchymal changes during early focal cerebral
449 ischemia and reperfusion. *Stroke.* 1994;25(9):1847-1853; discussion 1853-1854.
450 doi:10.1161/01.str.25.9.1847
- 451 15. El Amki M, Glück C, Binder N, et al. Neutrophils Obstructing Brain Capillaries Are a
452 Major Cause of No-Reflow in Ischemic Stroke. *Cell Rep.* 2020;33(2):108260.
453 doi:10.1016/j.celrep.2020.108260
- 454 16. Rayasam A, Hsu M, Kijak JA, et al. Immune responses in stroke: how the immune
455 system contributes to damage and healing after stroke and how this knowledge could be
456 translated to better cures? *Immunology.* 2018;154(3):363-376. doi:10.1111/imm.12918
- 457 17. Lin YH, Liu HM. Update on cerebral hyperperfusion syndrome. *J Neurointerventional*
458 *Surg.* 2020;12(8):788-793. doi:10.1136/neurintsurg-2019-015621
- 459 18. Fisher JA, Venkatraghavan L, Mikulis DJ. Magnetic Resonance Imaging-Based
460 Cerebrovascular Reactivity and Hemodynamic Reserve. *Stroke.* 2018;49(8):2011-2018.
461 doi:10.1161/STROKEAHA.118.021012
- 462 19. Sobczyk O, Battisti-Charbonney A, Fierstra J, et al. A conceptual model for CO2-
463 induced redistribution of cerebral blood flow with experimental confirmation using
464 BOLD MRI. *NeuroImage.* 2014;92:56-68. doi:10.1016/j.neuroimage.2014.01.051
- 465 20. Fierstra J, Sobczyk O, Battisti-Charbonney A, et al. Measuring cerebrovascular
466 reactivity: what stimulus to use? *J Physiol.* 2013;591(23):5809-5821.
467 doi:10.1113/jphysiol.2013.259150
- 468 21. van Niftrik CHB, Sebök M, Wegener S, et al. Increased Ipsilateral Posterior Cerebral
469 Artery P2-Segment Flow Velocity Predicts Hemodynamic Impairment. *Stroke.*
470 2021;52(4):1469-1472. doi:10.1161/STROKEAHA.120.032848
- 471 22. Sebök M, Niftrik CHB van, Lohaus N, et al. Leptomeningeal collateral activation
472 indicates severely impaired cerebrovascular reserve capacity in patients with
473 symptomatic unilateral carotid artery occlusion. *J Cereb Blood Flow Metab Off J Int Soc*
474 *Cereb Blood Flow Metab.* 2021;41(11):3039-3051. doi:10.1177/0271678X211024373
- 475 23. Zaidat OO, Yoo AJ, Khatri P, et al. Recommendations on angiographic revascularization
476 grading standards for acute ischemic stroke: a consensus statement. *Stroke.*
477 2013;44(9):2650-2663. doi:10.1161/STROKEAHA.113.001972
- 478 24. Rankin J. Cerebral vascular accidents in patients over the age of 60. II. Prognosis. *Scott*
479 *Med J.* 1957;2(5):200-215. doi:10.1177/003693305700200504

- 480 25. Slessarev M, Han J, Mardimae A, et al. Prospective targeting and control of end-tidal
481 CO₂ and O₂ concentrations. *J Physiol.* 2007;581(3):1207-1219.
482 doi:<https://doi.org/10.1113/jphysiol.2007.129395>
- 483 26. Power JD, Mitra A, Laumann TO, Snyder AZ, Schlaggar BL, Petersen SE. Methods to
484 detect, characterize, and remove motion artifact in resting state fMRI. *NeuroImage.*
485 2014;84:320-341. doi:10.1016/j.neuroimage.2013.08.048
- 486 27. Niftrik CHB van, Piccirelli M, Bozinov O, et al. Iterative analysis of cerebrovascular
487 reactivity dynamic response by temporal decomposition. *Brain Behav.*
488 2017;7(9):e00705. doi:<https://doi.org/10.1002/brb3.705>
- 489 28. Liu CF, Hsu J, Xu X, et al. Digital 3D Brain MRI Arterial Territories Atlas. *Sci Data.*
490 2023;10(1):74. doi:10.1038/s41597-022-01923-0
- 491 29. Sobczyk O, Battisti-Charbonney A, Poublanc J, et al. Assessing cerebrovascular
492 reactivity abnormality by comparison to a reference atlas. *J Cereb Blood Flow Metab*
493 *Off J Int Soc Cereb Blood Flow Metab.* 2015;35(2):213-220.
494 doi:10.1038/jcbfm.2014.184
- 495 30. Liu CF, Hsu J, Xu X, et al. Deep learning-based detection and segmentation of diffusion
496 abnormalities in acute ischemic stroke. *Commun Med.* 2021;1:61. doi:10.1038/s43856-
497 021-00062-8
- 498 31. Hernández-Pérez M, Werner M, Remollo S, et al. Early and Delayed Infarct Growth in
499 Patients Undergoing Mechanical Thrombectomy: A Prospective, Serial MRI Study.
500 *Stroke.* Published online November 3, 2022. doi:10.1161/STROKEAHA.122.039090
- 501 32. Kosior JC, Buck B, Wannamaker R, et al. Exploring Reperfusion Following
502 Endovascular Thrombectomy. *Stroke.* 2019;50(9):2389-2395.
503 doi:10.1161/STROKEAHA.119.025537
- 504 33. Potreck A, Mutke MA, Weyland CS, et al. Combined Perfusion and Permeability
505 Imaging Reveals Different Pathophysiologic Tissue Responses After Successful
506 Thrombectomy. *Transl Stroke Res.* 2021;12(5):799-807. doi:10.1007/s12975-020-
507 00885-y
- 508 34. Gwak DS, Choi W, Shim DH, et al. Role of Apparent Diffusion Coefficient Gradient
509 Within Diffusion Lesions in Outcomes of Large Stroke After Thrombectomy. *Stroke.*
510 2022;53(3):921-929. doi:10.1161/STROKEAHA.121.035615
- 511 35. Nagaraja N, Forder JR, Warach S, Merino JG. Reversible diffusion-weighted imaging
512 lesions in acute ischemic stroke: A systematic review. *Neurology.* 2020;94(13):571-587.
513 doi:10.1212/WNL.00000000000009173
- 514 36. Binder NF, Amki ME, Glück C, et al. *Leptomeningeal Collaterals Regulate Reperfusion*
515 *in Ischemic Stroke.*; 2023:2023.02.25.529915. doi:10.1101/2023.02.25.529915
- 516 37. Garcia JH. The neuropathology of stroke. *Hum Pathol.* 1975;6(5):583-598.
517 doi:10.1016/s0046-8177(75)80043-8

518 38. Goyal M, Ospel JM, Menon B, et al. Challenging the Ischemic Core Concept in Acute
 519 Ischemic Stroke Imaging. *Stroke*. 2020;51(10):3147-3155.
 520 doi:10.1161/STROKEAHA.120.030620

521

522

523 **TABLES**

Baseline demographics	All (n = 21)
Age	
Mean ± SD	69 ± 15
Year group	
<50	3 (14%)
50-70	8 (38%)
>70	10 (48%)
Sex	
M	9 (43%)
F	12 (57%)
Diseased vessel	
ICA	2 (10%)
MCA (M1/M2 segment)	11 (52%)
Both	8 (38%)
Clinical score at hospital admission	
NIHSS	
Median [IQR]	10.00 [8.00-16.00]
mRS	
Median [IQR]	4.00 [3.00-5.00]
Comorbidities	
Atrial fibrillation	4 (20%)
Smoking history	5 (24%)
Hypertension	13 (55%)
Dyslipidemia	8 (40%)
Obesity	3 (15%)
Diabetes	1 (5%)
Acute reperfusion therapy	
IVT	10 (50%)
EVT	21 (100%)
Symptom-to-needle time	
<4.5 hours	12 (57%)
>4.5 hours	2 (10%)
Wake-up stroke	7 (33%)
mTICI grade	
2b	5 (24%)
2c	3 (14%)
3	13 (62%)
Symptom-to-MR time	
<24 hours	3 (30%)
24-48 hours	11 (40%)
48-72 hours	7 (30%)
DWI infarct lesion [mL]	
Median [IQR]	26.30 [14.58-52.84]

524

525

Table 1. Baseline characteristics.

526 ICA indicates internal carotid artery; MCA, middle carotid artery; NIHSS, National Institutes of
 527 Health Stroke Scale; mRS, modified Ranking Scale; mTICI, modified Thrombolysis in Cerebral
 528 Infarction; IVT, intravenous thrombolysis; EVT, endovascular thrombectomy; MR, magnetic
 529 resonance; DWI, diffusion-weighted imaging.

530

531

532

533

Subject	Mean BOLD-CVR in MCA territory	Mean BOLD-CVR in ACA territory	Mean \pm SD BOLD-CVR in DWI lesion	DWI infarct lesion volume	SP volume in ACA + MCA territory	SP volume in DWI lesion	SP volume outside DWI lesion
1	0.07	0.11	0.04 \pm 0.01	10.18	14.94	3.84	11.09
2	0.09	0.07	0.02 \pm 0.01	14.58	42.64	6.42	36.22
3	0.08	0.14	0.06 \pm 0.01	47.15	4.40	0.70	3.70
4	0.11	0.09	0.08 \pm 0.01	2.02	2.71	0.06	2.65
5	0.06	0.08	0.01 \pm 0.01	97.12	189.76	73.84	115.92
6	-0.03	-0.01	-0.03 \pm 0.02	117.29	174.03	73.75	100.28
7	0.08	0.06	-0.03 \pm 0.02	72.13	129.37	45.88	83.49
8	0.08	0.06	0.06 \pm 0.01	26.30	8.77	1.24	7.54
9	0.12	0.08	0.04 \pm 0.01	13.89	4.07	1.34	2.73
10	0.14	0.12	0.08 \pm 0.01	4.29	2.59	0.00	2.60
11	0.19	0.23	0.09 \pm 0.02	18.00	21.58	2.79	18.78
12	0.15	0.20	0.03 \pm 0.03	36.41	42.69	19.34	23.35
13	0.08	0.08	-0.01 \pm 0.01	89.57	83.99	51.79	32.20
14	0.06	0.00	0.03 \pm 0.01	17.74	25.79	3.28	22.51
15	0.20	0.14	0.17 \pm 0.02	1.33	0.36	0.00	0.36
16	0.06	0.15	-0.05 \pm 0.01	52.84	113.19	46.55	66.64
17	0.04	0.05	-0.04 \pm 0.02	23.30	57.50	17.92	39.57
18	0.13	0.10	0.08 \pm 0.01	30.78	18.49	4.97	13.52
19	0.18	0.13	0.13 \pm 0.02	16.18	9.51	2.11	7.40
20	0.11	0.10	0.05 \pm 0.01	80.20	33.94	21.05	12.89
21	0.14	0.12	0.08 \pm 0.01	30.30	4.08	0.59	3.49

534

535 **Table 2. Distribution of BOLD-CVR associated steal phenomenon in the affected hemisphere.**

536 BOLD-CVR values are reported with unit [% Δ BOLD/mmHg]; volumes are reported with unit [mL];

537 BOLD-CVR indicates blood oxygen level dependent cerebrovascular reactivity; SP, steal
538 phenomenon; GM, grey matter; WM, white matter; ACA, anterior cerebral artery; MCA, middle
539 cerebral artery; PCA, posterior cerebral artery.

540

Variable	β	95% confidence interval (95-CI)	P value
Intercept	2.34	-5.57 to 10.25	0.540
Age	-0.06	-0.17 to 0.04	0.223
BOLD-CVR associated SP outside the infarct lesion (mL)	0.07	0.01 to 0.14	0.034*
DWI infarct lesion volume (mL)	0.03	-0.03 to 0.10	0.260
NIHSS at hospital admission	0.23	-0.06 to 0.53	0.116

541

542 **Table 3. Results of the linear regression model of the association between BOLD-CVR associated**
543 **steal phenomenon volume outside the infarct lesion and NIHSS score value at hospital discharge.**

544 β indicates the regression coefficient; BOLD-CVR, blood oxygen level dependent cerebrovascular
545 reactivity; SP, steal phenomenon; DWI, diffusion-weighted imaging; NIHSS, National Institutes of
546 Health Stroke Scale.

Study population

Patients with acute ischemic IVC stroke of the anterior circulation included in the MPACT cohort study that were successfully treated with rT (nT) (n = 76) and that received the pre-defined modified mRS examination within 72 hours from symptom onset.

Inclusion period: 03/2019 – 02/2022

n = 30

Missing HCl T2*WI data, n = 4

Patients that received mRS-CWR examination within 72 hours from successful rT

n = 76

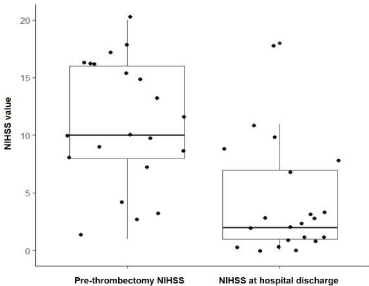
Excluded from the analysis
(n = 5)

- Excessive subject's head movement during mRS examination, n = 5

Included in the study analysis

Association between HCl T2*WI signal phenomenon (measured in the affected hemisphere) and DWI infarct lesion

n = 21



BOLD-CVR
map

BOLD-CVR associated
steal phenomenon

DWI infarct
lesion

(A)



(B)



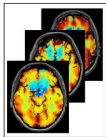
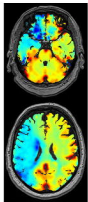
(C)



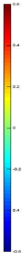
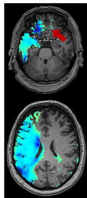
(D)



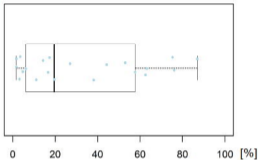
b1000



$$\text{CVR} < 0 \rightarrow \text{Z-score} = \frac{\text{CVR}_i - \text{Mean}_{ATLAS}}{\sigma_{ATLAS}}$$



(A)



(B)

